





Sports Simulation Scheme based on Artificial Intelligence-assisted Agile Internet of Things

Long Wang¹ and Shuping Xu^{1*}

¹Physical Education Department of North China Electric Power University, Beijing 102206, China
longwang1988@163.com, 13601259375@163.com

Corresponding author: Shuping Xu, 13601259375@163.com

Abstract. In order to improve the effect of sports strategy formulation, this paper combines artificial intelligence assisted agile Internet of Things to conduct research on sports simulation scheme, and builds an intelligent sports simulation system. The sports simulation model designed in this paper can change the mechanism parameters according to the actual situation of the moving object, establish the fixed coordinate system and local coordinate system of the parallel platform model, and establish the mathematical model of the parallel platform. Moreover, according to the principle of vector closure, the inverse kinematics position solution is analyzed, and the inverse kinematic velocity solution is derived by using the equation of the inverse position solution. The experimental research results show that the sports simulation system based on artificial intelligence-assisted agile Internet of Things proposed in this paper has a good performance in sports simulation.

Keywords: artificial intelligence; agile Internet of things; sports; simulation

DOI: <https://doi.org/10.14733/cadaps.2023.S12.1-21>

1 INTRODUCTION

The concept of "smart city" refers to the use of cloud computing, big data, Internet of Things and mobile Internet and other information technologies to manage, monitor, process and analyze massive amounts of information. At the same time, it makes timely, accurate, effective and guaranteed responses to various needs including people's livelihood, environmental protection, public safety, urban services, and industrial and commercial activities. Its essence is to realize the intelligent management and operation of the city, to serve people more conveniently, and to promote the harmonious and sustainable growth of the city. Its main core is people. There are three most basic elements: networking, digitization and intelligence. That is to say, "wisdom" needs to be based

on digitalization, networked as the condition, and intelligent as the core. The interaction between the three is better and more convenient for operation and management, so as to serve people.

Digitization-based means that in the traditional physical world, things in the physical world can be transformed into readable values in the information world through the perception of sensors, and presented in the information world, one by one with the things in the physical world. Correspondingly, operations and processing can be performed through data processing analysis. Networking is a condition. Even if information is related to information, the information that has no connection itself is linked together through the Internet, and then through the combination of the Internet of Things and the Internet, things (including people) in the traditional physical world are connected with information, information and information. Get full access. The core of intelligence is to rely on science and technology to realize the fundamental, the digital resource information can be stored, and through the background operation, the more reasonable decision-making makes the management easier, and everything becomes more intelligent. Analysis and decision-making become intelligent insights. It can be said that the fundamental purpose of the development of "smart city" is to make people's life and production more convenient, and to serve people with higher quality.

The concept of sports is broadly called sports. It is a conscious and organized social activity aimed at enhancing people's physical fitness, promoting people's all-round development, enriching social and cultural life and promoting spiritual civilization with physical exercises as the basic means [8]. In a narrow sense, it is called physical education, which is an educational process that develops the body, strengthens the physique, imparts the knowledge and skills of physical exercise, and cultivates the moral and volitional qualities. The basic structure is composed of social sports, school sports and competitive sports. The "wisdom" in the city is more manifested in the convenience of people's life and production, so the "wisdom" in sports is also the same. In addition, it is a convenient way to meet people's needs for physical fitness and sports entertainment in their leisure time [6]. People's demand for sports stems from the desire for health, so in this paper, the sports in "smart sports" refers to a convenient way to obtain physical fitness and sports entertainment [17].

This paper combines artificial intelligence-assisted agile Internet of Things to carry out the research on sports simulation scheme, constructs an intelligent sports simulation system, effectively improves the effect of physical exercise simulation, and provides a theoretical reference for the formulation of post-sports fitness programs.

2 RELATED WORK

The Internet of Things (IoT) is predicted to be another wave of technology and economy in the global information industry after the Internet, and has been paid attention to by governments, enterprises and academia in various countries. strategy [15]. Compared with technologically advanced countries, my country is not far behind in the field of Internet of Things. The Internet of Things involves automatic control, information sensing, radio frequency identification, wireless communication and computer technology. With the decline in the cost of processors, memory, network bandwidth, etc., the Internet of Things has been applied in the fields of warehousing and logistics[4], prevention of counterfeit products, infrastructure such as smart buildings, street light management, smart meters, urban water networks, and medical care[11]. IoT technology also faces many challenges, such as providing secure and real-time data service technology, correctness verification technology of IoT system, embedded World Wide Web service development technology, privacy protection technology and security control technology, etc. Whether it can be widely used key technology [16]. If these technologies can be conquered, it is certain that in the context of my country's vigorous promotion of the integration of industrialization and informatization, the Internet of Things will be an important technological development engine in the informatization process of industry and even more industries [14]. It has been confirmed by means of mobile phone data

collection and two-dimensional code identification that the integration of mobile Internet and traditional Internet of Things has produced wider applications. In the near future, we will enter the era of Internet of Things [5]. .

The emphasis on sports simulation is relatively high, and the research also has depth and breadth. However, from the perspective of the running effect of sports simulation, it has not yet reached the ideal state. Constrained by the cumbersome process of sports simulation, complicated testing, and lack of guidance, the awareness, participation and follow-up fitness guidance of sports simulation all over the country are lacking to varying degrees [1]. The simplification and isolation of sports simulation models are one of the reasons for these problems [10]. How to closely link sports simulation with our daily life, become a part of our way of life, and integrate with our other behavioral habits, requires serious research and discussion, and we believe that the integration of sports simulation and Internet of Things technology one of the development trends. The most important concept in IoT development is fusion [7]. The Internet of Things realizes service integration and business integration through device integration, network integration, and platform integration, combining sports simulation with smart phones, social incentives and other fashionable lifestyles. With the vigorous rise of technologies such as the Internet of Things and the mobile Internet, sports simulation is integrated with the mobile Internet carrier represented by smartphones, as well as the Internet of Things and other modern scientific information technologies characterized by identification, etc., to research and develop a set of The national physique monitoring system with the dual genes of the Internet of Things and the mobile Internet is of great significance [3].

In terms of data acquisition equipment, there are currently some fitness equipment with built-in dashboards on the market. These equipment can provide data such as fitness parameters and operating parameters by themselves. For example, common treadmills output speed, slope and other information through a serial interface. With the help of the instrument panel that comes with the device to collect various exercise parameters, it is only necessary to design a data transmission unit based on the IO interface of the instrument panel and the agreed data transmission protocol, and then the data of this type of fitness equipment can be collected and summarized. , and transmitted to the central computer through the local area network. For fitness equipment without a dashboard, we collect exercise parameters by deploying wireless sensors, and design a local fitness guidance terminal to achieve summary, upload, visualization and equipment management of exercise parameters. On this basis, a central computer is designed, which realizes data uploading to a remote server, and integrates functional modules such as personnel management, equipment management, and remote data query and visualization [12]. Design a three-level integrated fitness monitoring network of fitness terminal or data transmission unit→central computer→remote server. Therefore, at the fitness terminal or data transmission unit layer, it is necessary to upload data in a unified format to the central computer according to the agreed format [13]; at the central computer layer, it is necessary to monitor the status of the equipment, and at the same time, it is necessary to collect fitness data according to the agreed format. The data and statistics are transmitted to the remote server according to the agreed format. On the other hand, the information broadcast by the remote server needs to be parsed and visualized to display functions such as data query and fitness guidance. At the remote server layer, it is necessary to collect motion parameters according to the agreed format, and at the same time broadcast messages to the central computer according to the relevant protocols to provide related services [21].

3 SPORTS SIMULATION BASED ON AGILE IOT

The sports simulation model designed in this paper can change the parameters of the mechanism according to the actual situation of the moving object, and its mechanism diagram and coordinate system definition are shown in figure 1. A_1 , A_2 , A_3 , and A_4 are the four connection points

between the active traction force and the moving platform, and $P_i(i=1,2\dots6)$ is the connection point between the traction force and the static platform. Among them, $P_i(i=1,2,3,4)$ is in the same horizontal plane, the distance between it and the bottom surface is 1000mm , and the distance between $P_i(i=5,6)$ and the bottom surface is 1500mm . At the initial position, the traction force $A_iP_i(i=1,2,3,4)$ is in the same horizontal plane as the moving platform, and Q corresponds to the center point of the pelvis. The functions of the six traction force A_iP_i (A_5, A_6 coincide with A_2 and A_4 respectively) are distributed as follows: The movement of 1R2T in the horizontal plane is realized by pulling the $A_iP_i(i=1-4)$ force, and the 1T movement in the vertical direction is realized by pulling the $A_iP_i(i=5-6)$ force and gravity. In the specific motion control, the six active traction forces jointly drive the motion of the moving platform to perform sports on the moving object.

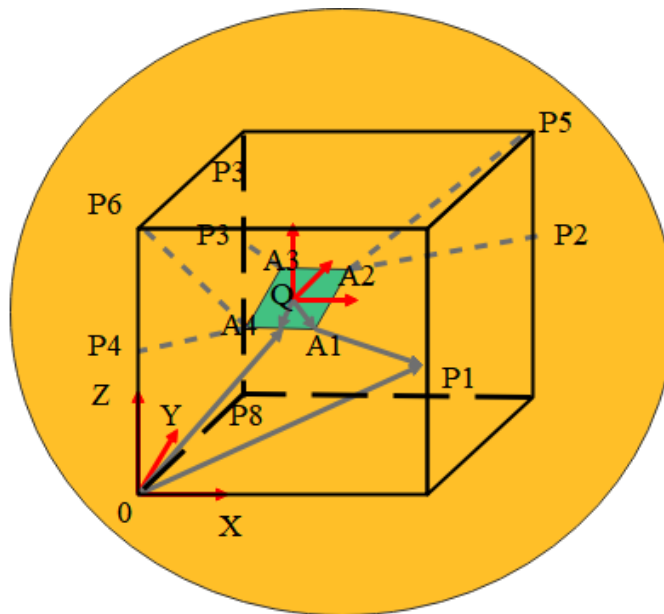


Figure 1: Sketch of the traction-driven sports simulation model and the definition of the coordinate system.

The coordinate origin of the fixed coordinate system OXYZ coincides with the O point, the positive direction of the X axis is along the $\overrightarrow{OP_7}$ direction, the positive direction of the Y axis is along the $\overrightarrow{OP_8}$ direction, and the positive direction of the Z axis is along the $\overrightarrow{OP_6}$ direction. The coordinate origin of the local coordinate system Qxyz coincides with the Q point, the positive direction of the X axis is along the $\overrightarrow{QB_1}$ direction (point B_1 is the midpoint of A_1A_2), the positive direction of the Y

axis is along the $\overline{QB_2}$ direction (point B_2 is the midpoint of A_2A_3), and the positive direction of the Z axis is straight upward. The coordinates of the connection point $P_i (i=1,2\dots6)$ between the traction force and the static platform in the fixed coordinate system are: $P_1(740,120,1000), P_2(1135,690,1000), P_3(540,1435,1000), P_4(145,890,1000), P_5(1135,790,1500), P_6(145,790,1500)$. At the initial position, the coordinates of the connection point $A_i (i=1,2,3,4)$ between the traction force and the moving platform in the local coordinate system are: $A_1(0,-100,0), A_2(100,0,0), A_3(0,100,0), A_4(100,0,0)$. In the subsequent modeling process, we assume that the traction force is taut and inelastic, and gravity is ignored.

The inverse kinematic position solution is: knowing the position vector $\overline{OQ} = (x, y, z)^T$ of the Q point on the moving platform in the fixed coordinate system and the angle θ that the moving platform rotates around the Z axis and the positive direction of the X axis, the length L_i of the six traction forces can be calculated. Since the winding module and the guide pulley are fixed on the fixed frame, the positional relationship between them remains unchanged during the movement of the moving platform, and the changed part is the change in rope length between the guide pulley and the moving platform. For this reason, in the kinematic inverse solution model for calculating the traction force-driven sports simulation model, it is only necessary to calculate the relationship between the change of the traction force length between the guide pulley and the moving platform and the pose of the moving platform. In the following, starting from the specific structure of the robot, the inverse kinematics position analysis is carried out with the hinge connection points on the static platform and the moving platform and the spatial positional relationship between them as the research objects.

We assume that $\overline{OP_i} (i=1,2\dots6)$ is the position vector of point P_i in the fixed coordinate system, $\overline{L_i} = \overline{A_iP_i} (i=1,2\dots6)$ is the traction force vector, and $\overline{QA_i} (i=1,2\dots6)$ is the position vector of point A_i in the local coordinate system. Then, the following rotation matrix can be obtained from the closed vector quadrilateral method and the coordinate transformation relationship of robotics[9]:

$$\overline{L_i} = \overline{OP_i} - \overline{OQ} - {}^o\mathbf{R}\overline{QA_i} (i=1,2\dots6) \quad (3.1)$$

Formula (3.1) is written in matrix form:

$$\overline{L_i} = \mathbf{TB}_i (i=1,2\dots6) \quad (3.2)$$

Among them, there are:

$$\mathbf{T} = \begin{bmatrix} \mathbf{E} & {}^0\mathbf{R} & -\mathbf{E} \end{bmatrix}_{3 \times 9} \quad (3.3)$$

$$\mathbf{B}_i = \begin{bmatrix} \overrightarrow{OP_i} \\ \overrightarrow{QA_i} \\ \overrightarrow{OQ} \end{bmatrix}_{9 \times 1} \quad (i=1,2\dots6) \quad (3.4)$$

The length of the i-th traction force is:

$$L_i = \|\vec{L}_i\| = \|\overrightarrow{A_i P_i}\| \quad (i=1,2\dots6) \quad (3.5)$$

In this paper, according to the specific motion trajectory of the pelvis, the simulation calculation of the length, speed and acceleration of the traction force is carried out. The above specific calculation formula provides the mathematical model of each module for the subsequent simulation work.

Since the vectors $\overrightarrow{OP_i}$ and $\overrightarrow{QP_i}$ are constants, we have:

$$\frac{d}{dt} \overrightarrow{OP_i} = 0, \frac{d}{dt} \overrightarrow{QA_i} = 0 \quad (3.6)$$

The derivative formula of the rotation matrix of the robot is:

$$\frac{d}{dt} {}^o \mathbf{R} = \mathbf{S}(\omega) {}^o \mathbf{R} = \boldsymbol{\omega} \times {}^o \mathbf{R} \quad (3.7)$$

Among them, $\mathbf{S}(\omega)$ is the angular velocity operator matrix, as follows:

$$\mathbf{S}(\omega) = \begin{bmatrix} 0 & -\omega_z & \omega_y \\ \omega_z & 0 & -\omega_x \\ -\omega_y & \omega_x & 0 \end{bmatrix} \quad (3.8)$$

From formulas (3.6) and (3.7), it can be obtained[3.2]:

$$\frac{d}{dt} ({}^o \mathbf{R} \cdot \overrightarrow{QA_i}) = \frac{d}{dt} {}^o \mathbf{R} \cdot \overrightarrow{QA_i} + {}^o \mathbf{R} \cdot \frac{d}{dt} \overrightarrow{QA_i} = \frac{d}{dt} {}^o \mathbf{R} \cdot \overrightarrow{QA_i} = (\boldsymbol{\omega} \times {}^o \mathbf{R}) \cdot \overrightarrow{QA_i} \quad (3.9)$$

We take derivation on both sides of formula (3.5), and substitute formulas (3.6), (3.7), (3.9) into it, we can get:

$$\begin{aligned}
\dot{L}_i &= \frac{d}{dt} \|\bar{L}_i\| = \frac{1}{\|\bar{L}_i\|} \frac{d}{dt} \left[\frac{1}{2} \|\bar{L}_i\|^2 \right] = \frac{1}{2\|\bar{L}_i\|} \frac{d}{dt} \left[\|\overline{OP}_i - \overline{OQ} - {}^o\mathbf{RQA}_i\|^2 \right] \\
&= \frac{1}{2\|\bar{L}_i\|} \frac{d}{dt} \left[\overline{OP}_i \cdot \overline{OP}_i + \overline{OQ} \cdot \overline{OQ} + ({}^o\mathbf{RQA}_i) \cdot ({}^o\mathbf{RQA}_i) \right. \\
&\quad \left. - 2\overline{OP}_i \cdot \overline{OQ} - 2\overline{OP}_i \cdot ({}^o\mathbf{RQA}_i) + 2\overline{OQ} \cdot ({}^o\mathbf{RQA}_i) \right] \\
&= \frac{1}{2\|\bar{L}_i\|} \left[2\overline{OP}_i \cdot \frac{d}{dt} \overline{OP}_i + 2\overline{OQ} \cdot \frac{d}{dt} \overline{OQ} + 2({}^o\mathbf{RQA}_i) \cdot \frac{d}{dt} ({}^o\mathbf{RQA}_i) - 2 \frac{d\overline{OP}_i}{dt} \cdot \overline{OQ} \right. \\
&\quad \left. - 2\overline{OP}_i \cdot \frac{d}{dt} \overline{OQ} - 2 \frac{d\overline{OP}_i}{dt} \cdot ({}^o\mathbf{RQA}_i) - 2\overline{OP}_i \cdot \frac{d}{dt} ({}^o\mathbf{RQA}_i) \right. \\
&\quad \left. + 2 \frac{d\overline{OQ}}{dt} \cdot ({}^o\mathbf{RQA}_i) + 2\overline{OQ} \cdot \frac{d}{dt} ({}^o\mathbf{RQA}_i) \right] \\
&= \frac{1}{\|\bar{L}_i\|} \left[0 + \overline{OQ} \cdot \overline{OQ} + ({}^o\mathbf{RQA}_i) \cdot \left(\frac{d}{dt} {}^o\mathbf{RQA}_i \right) - 0 - \overline{OP}_i \cdot \overline{OQ} - 0 - \overline{OP}_i \cdot \left(\frac{d}{dt} {}^o\mathbf{RQA}_i \right) \right. \\
&\quad \left. + \overline{OQ} \cdot ({}^o\mathbf{RQA}_i) + \overline{OQ} \cdot \left(\frac{d}{dt} {}^o\mathbf{RQA}_i \right) \right] \\
&= \frac{1}{\|\bar{L}_i\|} \left[(\overline{OQ} - \overline{OP}_i + {}^o\mathbf{RQA}_i) \cdot \overline{OQ} + ({}^o\mathbf{RQA}_i - \overline{OP}_i + \overline{OQ}) \cdot \left(\frac{d}{dt} ({}^o\mathbf{RQA}_i) \right) \right] \\
&= \frac{1}{\|\bar{L}_i\|} \left[-\bar{L}_i \cdot \overline{OQ} - \bar{L}_i \cdot (\boldsymbol{\omega} \times {}^o\mathbf{RQA}_i) \right] = \frac{1}{\|\bar{L}_i\|} \left[-\bar{L}_i \cdot \overline{OQ} - ({}^o\mathbf{RQA}_i \times \bar{L}_i) \cdot \boldsymbol{\omega} \right] \\
&= \mathbf{U}_i \cdot \overline{OQ} + ({}^o\mathbf{RQA}_i \times \mathbf{U}_i) \cdot \boldsymbol{\omega} = \begin{bmatrix} \mathbf{U}_i^T & ({}^o\mathbf{RQA}_i \times \mathbf{U}_i)^T \end{bmatrix} \begin{bmatrix} \overline{OQ} \\ \boldsymbol{\omega} \end{bmatrix} \quad (i=1,2,\dots,6) \quad (3.10)
\end{aligned}$$

$$\overline{OQ} = \frac{d}{dt} \overline{OQ}$$

Among them, \overline{OQ} is the linear velocity of the center point of the pelvis of the moving platform, $\boldsymbol{\omega}$ is the angular velocity of the pelvis of the moving platform, \mathbf{U}_i is the unit vector of the i -th traction force length, and its direction is opposite to the direction of the traction force vector, which can be written as the expression:

$$\mathbf{U}_i = -\frac{\dot{L}_i}{L_i} \vec{L}_i \quad (3.11)$$

We set the position vector of point A_i in the fixed coordinate system as $\vec{P}_{A,i}$, and the velocity of point A_i as $\dot{\vec{P}}_{A,i}$, then we have:

$$\vec{P}_{A,i} = \vec{OQ} + {}^o\mathbf{R}\vec{QA}_i \quad (3.12)$$

Taking the derivation of both ends of formula (3.12), we can get:

$$\dot{\vec{P}}_{A,i} = \vec{OQ} + {}^o\mathbf{R} \frac{d}{dt} \vec{QA}_i + \mathbf{S}(\omega) {}^o\mathbf{R} \vec{QA}_i = \vec{OQ} + \omega \times ({}^o\mathbf{R} \vec{QA}_i) \quad (3.13)$$

Multiplying both ends of formula (3.13) by \mathbf{U}_i , we can get:

$$\mathbf{U}_i \cdot \dot{\vec{P}}_{A,i} = \mathbf{U}_i^T \vec{OQ} + \mathbf{U}_i^T \omega \times ({}^o\mathbf{R} \vec{QA}_i) \quad (3.14)$$

From the above formula, we can get:

$$\mathbf{U}_i \cdot \dot{\vec{P}}_{A,i} = \mathbf{U}_i^T \vec{OQ} + ({}^o\mathbf{R} \vec{QA}_i \times \mathbf{U}_i)^T \omega \quad (3.15)$$

Therefore, there are

$$\dot{L}_i = \mathbf{U}_i \cdot \dot{\vec{P}}_{A,i} \quad (3.16)$$

Since \mathbf{U}_i is the unit vector of the i-th traction force, we have:

$$\|\dot{L}_i\| \leq \|\dot{\vec{P}}_{A,i}\| \quad (3.17)$$

This means that the speed of the traction force is equal to the projection of the speed of the hinge point of the corresponding moving platform in the direction of the rope. Therefore, the speed of the traction force is always less than or equal to the speed of the hinge point of the corresponding moving platform.

The 6 formulas obtained by formula (3.10) can be written in matrix form as follows:

$$\dot{\mathbf{L}} = \mathbf{A}^T \dot{\mathbf{X}} \quad (3.18)$$

Among them, $\dot{\mathbf{L}}$ is the velocity vector of the length change of the traction force, \mathbf{A}^T is the motion Jacobian matrix of the traction force-driven sports simulation model, and $\dot{\mathbf{X}}$ is the motion velocity vector of the pelvis on the moving platform. They are respectively represented by the following formulas:

$$\dot{\mathbf{L}} = [\dot{L}_1 \quad \dot{L}_2 \quad \cdots \quad \dot{L}_6]^T \quad (3.19)$$

$$\mathbf{A}^T = \begin{bmatrix} \mathbf{U}_1^T & \left({}^o\mathbf{R}\overline{\mathbf{QA}}_1 \times \mathbf{U}_1 \right)^T \\ \mathbf{U}_2^T & \left({}^o\mathbf{R}\overline{\mathbf{QA}}_2 \times \mathbf{U}_2 \right)^T \\ \vdots & \vdots \\ \mathbf{U}_6^T & \left({}^o\mathbf{R}\overline{\mathbf{QA}}_6 \times \mathbf{U}_6 \right)^T \end{bmatrix} \quad (3.20)$$

$$\dot{\mathbf{X}} = [\overline{OQ} \quad \boldsymbol{\omega}]^T \quad (3.21)$$

The above is the derivation of the motion Jacobian matrix of the sports simulation model. These derivation results lay the mathematical foundation for the subsequent MATLAB simulation and provide the basis for the simulation. From the expression of the motion Jacobian matrix of the traction force-driven sports simulation model, it can be seen that the motion Jacobian matrix of the traction force-driven sports simulation model is similar in form to the industrial robot and the rod-supported sports simulation model.

The physical meaning of derivation on both sides of $\dot{\mathbf{L}} = \mathbf{A}^T \dot{\mathbf{X}}$ is to solve the acceleration of rope length. From this, the inverse solution formula of acceleration can be obtained as:

$$\ddot{\mathbf{L}} = \mathbf{A}^T \ddot{\mathbf{X}} + \dot{\mathbf{A}}^T \dot{\mathbf{X}} \quad (3.22)$$

Taking the derivation of formula (16) $\dot{L}_i = \mathbf{U}_i \cdot \dot{\overline{P}}_{A,i}$, the acceleration of the i -th traction force can be obtained, and its formula is:

$$\ddot{L}_i = \mathbf{U}_i \ddot{\overline{P}}_{A,i} + \dot{\mathbf{U}}_i \cdot \dot{\overline{P}}_{A,i} \quad (3.23)$$

Differentiating both sides of formula (3.13), we get:

$$\begin{aligned} \ddot{\overline{P}}_{A,i} &= \overline{OQ} + \mathbf{S}(\dot{\omega}) {}^o\mathbf{R}\overline{\mathbf{QA}}_i + \mathbf{S}(\omega)\mathbf{S}(\dot{\omega}) {}^o\mathbf{R}\overline{\mathbf{QA}}_i + \mathbf{S}(\omega) {}^o\mathbf{R}\overline{\mathbf{QA}}_i \\ &= \overline{OQ} + \mathbf{S}(\dot{\omega}) {}^o\mathbf{R}\overline{\mathbf{QA}}_i + \mathbf{S}(\omega)\mathbf{S}(\omega) {}^o\mathbf{R}\overline{\mathbf{QA}}_i \end{aligned} \quad (3.24)$$

Substituting formulas (3.13) and (3.24) into formula (3.23), we can get:

$$\ddot{L}_i = \mathbf{U}_i \cdot \left(\overline{OQ} + \mathbf{S}(\dot{\omega}) {}^o\mathbf{R}\overline{\mathbf{QA}}_i + \mathbf{S}(\omega)\mathbf{S}(\omega) {}^o\mathbf{R}\overline{\mathbf{QA}}_i \right) + \dot{\mathbf{U}}_i \cdot \left(\overline{OQ} + \mathbf{S}(\omega) {}^o\mathbf{R}\overline{\mathbf{QA}}_i \right) \quad (3.25)$$

Differentiating both sides of formula (3.1), we can get

$$\dot{L}_i = \overline{OP}_i - \overline{OQ} \cdot {}^o\mathbf{R} \frac{d}{dt} \overline{QA}_i - S(\omega) {}^o\mathbf{R} \overline{QA}_i = -\overline{OQ} - S(\omega) {}^o\mathbf{R} \overline{QA}_i (i = 1, 2, \dots, 6) \quad (3.26)$$

Substituting formula (3.26) into formula (3.25), we get:

$$\begin{aligned} \ddot{L}_i &= \mathbf{U}_i \cdot \left(\overline{OQ} + \mathbf{S}(\dot{\omega}) {}^o\mathbf{R} \overline{QA}_i + \mathbf{S}(\omega) \mathbf{S}(\omega) {}^o\mathbf{R} \overline{QA}_i \right) + \frac{\dot{L}_i}{L_i} \cdot \left(\overline{OQ} + \mathbf{S}(\omega) {}^o\mathbf{R} \overline{QA}_i \right) \\ &= \mathbf{U}_i \cdot \left(\overline{OQ} + \mathbf{S}(\dot{\omega}) {}^o\mathbf{R} \overline{QA}_i + \mathbf{S}(\omega) \mathbf{S}(\omega) {}^o\mathbf{R} \overline{QA}_i \right) \\ &\quad - 1/L_i \left(\overline{OQ} \cdot \overline{OQ} + 2\overline{OQ} \cdot \left(\mathbf{S}(\omega) {}^o\mathbf{R} \overline{QA}_i \right) + \left(\mathbf{S}(\omega) {}^o\mathbf{R} \overline{QA}_i \right) \cdot \left(\mathbf{S}(\omega) {}^o\mathbf{R} \overline{QA}_i \right) \right) \end{aligned} \quad (3.27)$$

Among them, there are:

$$\mathbf{S}(\dot{\omega}) = \begin{bmatrix} 0 & -\dot{\omega}_z & \dot{\omega}_y \\ \dot{\omega}_z & 0 & -\dot{\omega}_x \\ -\dot{\omega}_y & \dot{\omega}_x & 0 \end{bmatrix} \quad (3.28)$$

Formula (3.27) is the solution formula for the acceleration of the i-th traction force, and the variation law of the acceleration cloud motion of the six traction forces can be obtained by using the formula (3-27). From the derivation formula of traction acceleration, it can be seen that the inverse solution of acceleration of parallel platforms is more complicated.

The correct kinematic position solution is: Knowing the lengths of the 6 traction forces, the position vector $\overline{OQ} = (x, y, z)^T$ of the Q point on the moving platform in the fixed coordinate system and the angle θ that the moving platform rotates around the Z axis and the positive direction of the X axis are solved. From formula (5), we can get:

$$\begin{cases} L_1 = \|\overline{A_1P_1}\| \\ L_2 = \|\overline{A_2P_2}\| \\ L_3 = \|\overline{A_3P_3}\| \\ L_4 = \|\overline{A_4P_4}\| \\ L_5 = \|\overline{A_5P_5}\| \\ L_6 = \|\overline{A_6P_6}\| \end{cases} \quad (3.29)$$

The above formula (3.29) is a nonlinear formula system, and there is often no analytical solution. In order to solve the roots of the system of formulas, the Newton-Raphson iteration method is generally used. The method linearizes the nonlinear formula, plugs it in with an initial guess, and iterates layer by layer, eventually producing a solution that is within the error tolerance.

The specific process of solving the nonlinear system of formulas by the Newton-Raphson iteration method is as follows:

The function can be constructed by formula (3.29):

$$F_i(\mathbf{X}) = \|\bar{L}_i\| - L_i (i = 1, 2 \dots 6) \quad (3.30)$$

By the Newton-Raphson iteration method, there are:

$$\mathbf{X}_{k+1} = \mathbf{X}_k + \delta\mathbf{X}_k \quad (3.31)$$

Among them, there are:

$$\delta\mathbf{X}_k = -\frac{F_i(\mathbf{X})}{\mathbf{J}_i} \quad (3.32)$$

That is :

$$\mathbf{J}_i \delta\mathbf{X}_k = -F_i(\mathbf{X}) \quad (3.33)$$

$$\mathbf{J}_i = \left[\begin{array}{cccc} \frac{\partial F_i(\mathbf{X})}{\partial x} & \frac{\partial F_i(\mathbf{X})}{\partial y} & \frac{\partial F_i(\mathbf{X})}{\partial z} & \frac{\partial F_i(\mathbf{X})}{\partial \theta} \end{array} \right]_{1 \times 4}, i = (1, 2 \dots 6) \quad (3.34)$$

Formula (3.33) is written in matrix form, that is:

$$\mathbf{J} \delta\mathbf{X}_k = -\mathbf{F}(\mathbf{X}) \quad (3.35)$$

Among them, there are:

$$\mathbf{J} = \begin{bmatrix} \mathbf{J}_1 \\ \mathbf{J}_2 \\ \mathbf{J}_3 \\ \mathbf{J}_4 \\ \mathbf{J}_5 \\ \mathbf{J}_6 \end{bmatrix} \quad \mathbf{F}(\mathbf{X}) = \begin{bmatrix} F_1(\mathbf{X}) \\ F_2(\mathbf{X}) \\ F_3(\mathbf{X}) \\ F_4(\mathbf{X}) \\ F_5(\mathbf{X}) \\ F_6(\mathbf{X}) \end{bmatrix} \quad (3.36)$$

The general formula for iterative solution is:

$$\delta\mathbf{X}_k = -\mathbf{J}^+ \mathbf{F}(\mathbf{X}) \quad (3.37)$$

The pseudo-inverse of the matrix \mathbf{J} is:

$$\mathbf{J}^+ = (\mathbf{J}^T \mathbf{J})^{-1} \mathbf{J}^T \quad (3.38)$$

Among them, $F_i(\mathbf{X})$ is the deviation function of the i -th traction force, \mathbf{X} is the pose matrix of the pelvis of the moving platform, δX_0 is the incremental value of the pose, and \mathbf{J}_i is the matrix of the partial derivative of $F_i(\mathbf{X})$ to the pose. At the beginning of the iteration, the algorithm firstly substitutes the guessed value $\mathbf{X}_0 = [x_0 \quad y_0 \quad z_0 \quad \theta_0]^T$ of the initial pose, obtains its incremental value $\delta \mathbf{X}_0$, and then repeatedly calculates and solves the formula (3.31) until $\|\delta \mathbf{X}_k\| < \xi$. The solution at this time is the approximate value of the positive kinematics solution, where ξ is a user-defined error tolerance.

In order to make up for the problem of loop iteration divergence that may be caused by improper selection of initial values, the author obtained the corresponding relationship between the length of traction force and the pose of the moving platform according to the inverse kinematics solution, and established a data table. When calculating the positive kinematics solution, the pose value of the moving platform corresponding to the length of the traction force can be found by looking up the table as the initial value of the iterative method.

Different training modes should be adopted in different stages of sports. In the initial stage of rehabilitation training, due to the small force that the lower limbs of the sports object can bear, in the initial stage, the sports object should be exercised under the condition of standing. Therefore, the motion type of the pelvis is planned as $1R2T$ in the horizontal plane (translation along the X axis, Y axis and rotation around the Z axis). The gravity of the human body is balanced by the passive protection cable and the active traction force $A_i P_i (i = 5 - 6)$, and the pelvis $1R2T$ motion type is realized by the active traction force $A_i P_i (i = 1 - 4)$, and the parallel mechanism type formed by it is a fully constrained parallel robot. Taking the above healthy male youth as an example, the motion trajectory formula of the pelvis when standing is defined as follows:

$$\begin{cases} x = 640 + 25 \sin(5t + \pi / 2) \\ y = 790 + 10 \sin(10t + \pi) \\ q = 4 \sin(5t) \end{cases} \quad (3.39)$$

In the formula, x and y are the coordinate values of the center point of the pelvis in the fixed coordinate system, and q is the rotation angle of the pelvis around the vertical axis.

4 RESEARCH ON SPORTS SIMULATION SCHEME BASED ON ARTIFICIAL INTELLIGENCE-ASSISTED AGILE INTERNET OF THINGS

Figure 2 shows the expected trajectory of the pelvic center point Q obtained by MATLAB programming when the sports simulation model-like motorized platform moves according to formula (38). Figures 3, 4, and 5 show the variation law of the length, speed, and acceleration of each active traction force calculated based on the inverse kinematics model when the sports simulation model-like motorized platform moves according to formula (38). In Figure 2, L_1, L_2, L_3, L_4 represents the length of the four active traction forces, in mm, and the simulation time t is 2s. In Figure 3, S_1, S_2, S_3, S_4

represents the speed of the four active traction forces, and the unit is mm/s . In Figure 4, a_1, a_2, a_3, a_4 represents the acceleration of the four active traction forces, and the unit is mm/s^2 . It can be seen from Figure 3, Figure 4, and Figure 5 that the length, velocity, and acceleration curves of the four active traction forces are continuous, and they all change with the pelvic movement as a sine or cosine function.

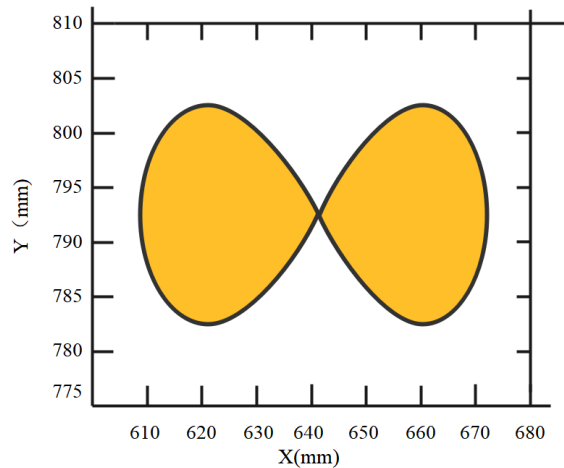


Figure 2: Desired trajectory of pelvic center point Q (when standing).

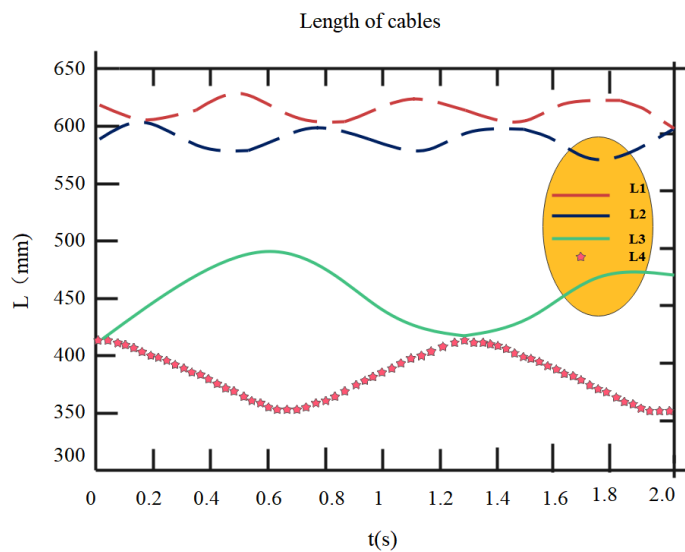


Figure 3: Variation of the length of each traction force when standing.

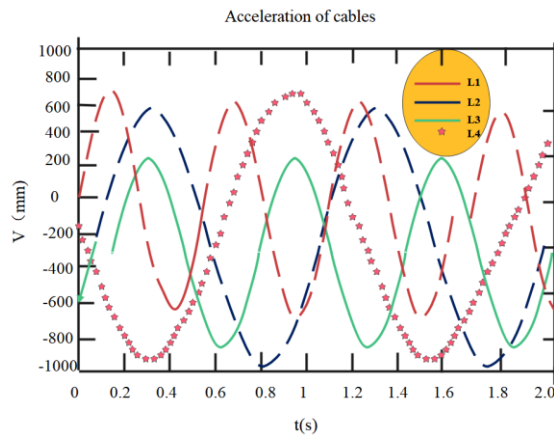


Figure 4: Variation law of each traction force speed when standing.

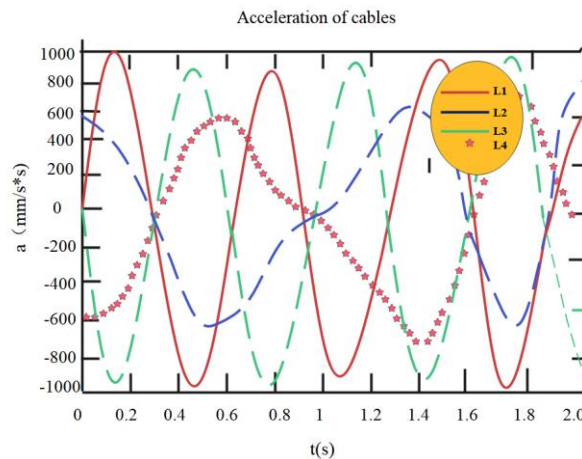


Figure 5: Variation law of acceleration of each traction force when standing.

In the later stage of sports, with the gradual recovery of the movement of the object's limbs, the lower limbs can bear a certain supporting force. For this reason, when exercising the moving object at this stage, the moving object should exercise during the gait process. As mentioned above, in the process of normal walking, the movement trajectory of the pelvis in the up-down, front-rear, and left-right directions approximates a sine curve. Taking the above healthy male youth as an example, the equation of the motion trajectory of the pelvis when walking is defined as follows:

$$\begin{cases} x = 640 + 25 \sin(5t + \pi / 2) \\ y = 790 + 10 \sin(10t + \pi) \\ z = 1000 + 10 \sin(10t + \pi / 2) \end{cases} \quad (4.1)$$

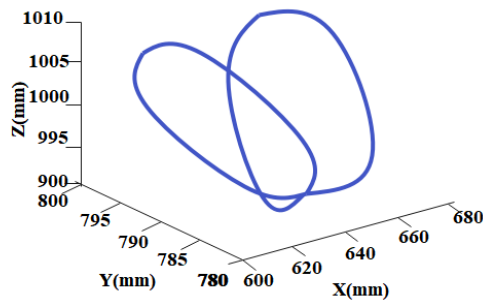
The velocity of the pelvic center point Q on the motion trajectory is:

$$\begin{cases} \dot{x} = 125 \cos(5t + \pi / 2) \\ \dot{y} = 100 \cos(10t + \pi) \\ \dot{z} = 100 \cos(10t + \pi / 2) \end{cases} \quad (4.2)$$

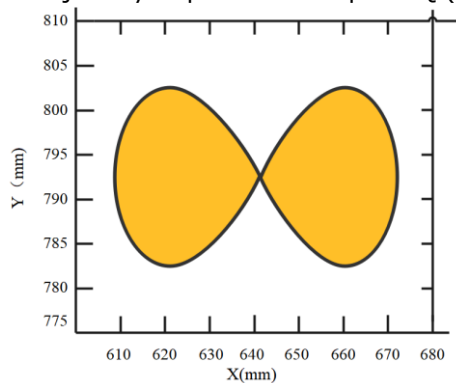
The acceleration of the pelvic center point Q on the motion trajectory is:

$$\begin{cases} \ddot{x} = -625 \sin(5t + \pi / 2) \\ \ddot{y} = -1000 \sin(10t + \pi) \\ \ddot{z} = -1000 \sin(10t + \pi / 2) \end{cases} \quad (4.3)$$

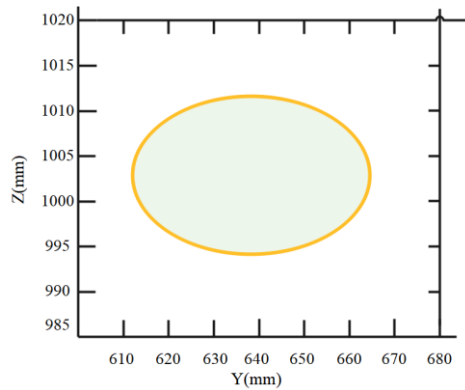
According to equation (3.39), the expected motion trajectory of the pelvic center Q point obtained by MATLAB programming is shown in Figure 6(a). The amplitudes of its movements along the X-axis, Y-axis, and Z-axis are 25mm, 10mm, and 10mm, respectively, and the initial moment of the gait cycle (calculated from the moment the right heel hits the ground). The pelvis reaches a maximum amplitude of 25mm in the left-right direction, the middle position in the front-back direction, and a maximum amplitude of 10mm in the up-down direction. Figure 6(b), Figure 6(c), Figure 6(d) are projections of the trajectory of Fig. 6(a) on three coordinate planes.



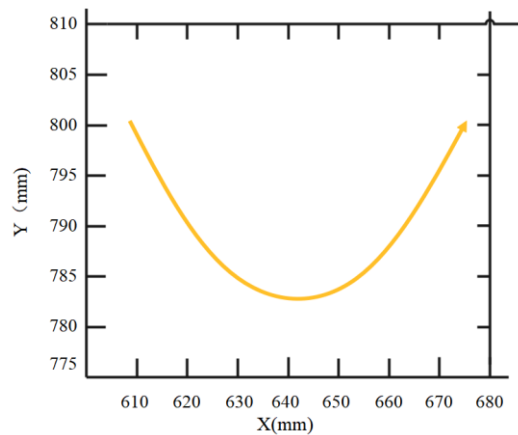
(a) Desired trajectory of pelvic center point Q (in gait)



(b) Projection of the desired trajectory of the pelvic center point Q on the XY plane



(c) Projection of the desired trajectory of the pelvic center point Q on the YZ plane



d) Projection of the desired trajectory of the pelvic center point Q on the XZ plane

Figure 6: Sports simulation projection.

In the actual system design and implementation, the sensing system and the central computer are connected through a wireless network, and the central computer acts as a fitness motion data sensing hub to collect, integrate and upload motion data in various applications. The perception system automatically collects sports fitness parameters and transmits them to the central computer through the wireless network. After the central computer receives the data, it integrates and counts the data, and saves and uploads the data to the remote server. The remote server performs data maintenance and central computer control, and the central computer manages and controls the fitness equipment. The IoT fitness system designed in this paper can be applied to a variety of different occasions. The network topology of the sports parameter monitoring used is shown in Figure 7.

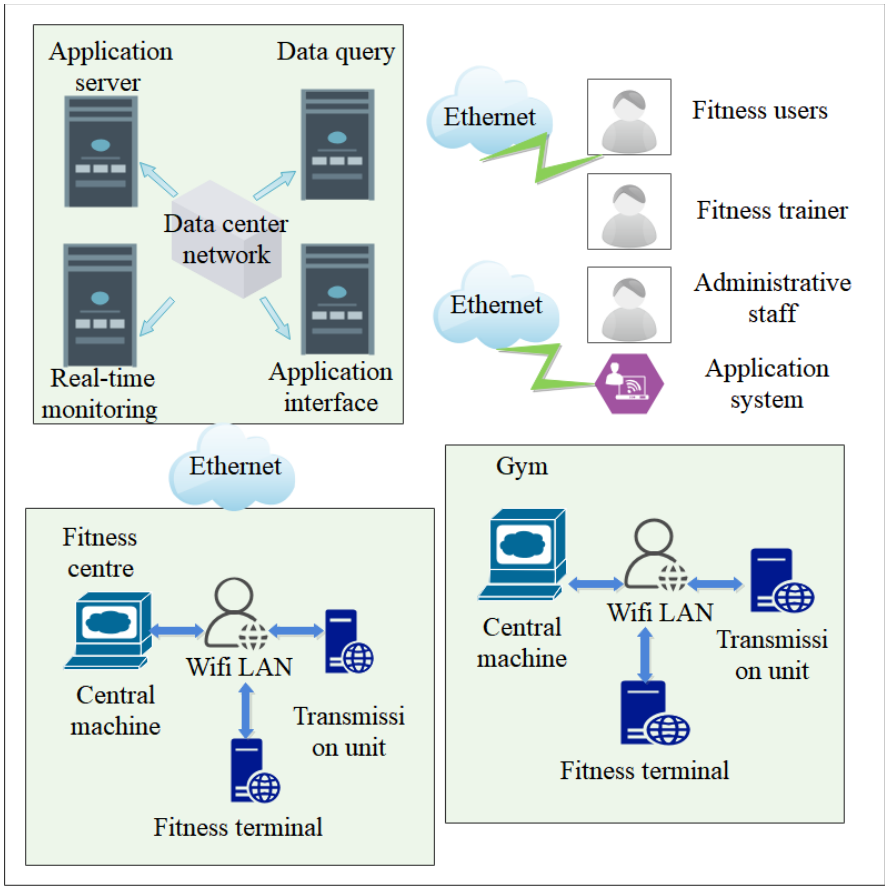


Figure 7: System network topology.

Figure 8 shows the sports simulation image based on AI agile IoT.



(a) Sports simulation character modeling



(b) Sports simulation image rendering



(c) Sports simulation reality map

Figure 8: Sports simulation image.

The perception layer of the sports simulation system of the Internet of Things plays the role of the collector of sports simulation information. It is compatible with various types of IoT sports simulation equipment through the perception layer central machine and gateway, and realizes all-weather LAN access and system access of various sports simulation equipment. In the perception layer, there are two main types of perception devices: data transmission units for self-contained dashboards and sports simulation terminals that match wireless sensors. Through the design and realization of the central computer to support the data transmission unit and the sports simulation terminal, the intelligent wireless sensor network system for the sports simulation of the Internet of Things is designed and realized. When deploying the perception layer equipment, the appropriate sports simulation equipment is selected according to the application of sports simulation, and the corresponding data transmission unit or wireless sensor and sports simulation terminal are designed to be connected to the center. The central computer has functions such as data acquisition and processing, network communication, authority management and human-machine interface, which need to be supported at the software and hardware levels of the central computer design. The center machine should be backward compatible with a variety of sports simulation equipment. Therefore,

it is necessary to design different data transmission units or wireless sensors and sports simulation terminals for different sports simulation equipment, so as to support different types of sports simulation equipment and realize the networking of equipment and data collection.

On the basis of the above construction model, this paper verifies the effect of the sports simulation system based on artificial intelligence-assisted agile Internet of Things proposed in this paper, counts the sports simulation effect of the model in this paper, and obtains the results shown in Table 1 below.

Table 1 Verification of the effect of the sports simulation system based on artificial intelligence-assisted agile IoT

<i>Number</i>	<i>Sports simulation</i>	<i>Number</i>	<i>Sports simulation</i>	<i>Number</i>	<i>Sports simulation</i>
1	84.1	25	81.3	49	90.5
2	82.5	26	85.9	50	87.2
3	83.5	27	83.9	51	84.1
4	88.5	28	80.2	52	90.9
5	89.2	29	86.7	53	86.7
6	83.5	30	89.0	54	83.6
7	85.1	31	83.5	55	90.2
8	80.6	32	86.5	56	82.1
9	82.7	33	82.0	57	84.9
10	89.4	34	84.1	58	84.0
11	88.2	35	83.1	59	90.9
12	84.9	36	82.1	60	82.9
13	81.6	37	90.7	61	85.8
14	83.2	38	89.7	62	85.2
15	90.1	39	80.3	63	83.3
16	89.7	40	84.7	64	80.0
17	84.0	41	85.8	65	83.5
18	90.8	42	89.1	66	84.1
19	90.2	43	81.1	67	80.2
20	85.7	44	89.1	68	82.5
21	82.3	45	83.8	69	86.2
22	81.5	46	80.7	70	87.3
23	85.6	47	88.6	71	81.0
24	86.6	48	82.7	72	90.8

Through the above research, it can be seen that the sports simulation system based on artificial intelligence-assisted agile Internet of Things proposed in this paper has a good performance in sports simulation.

5 CONCLUSION

The fundamental purpose of "smart sports" is to meet people's needs for physical fitness and leisure and entertainment, and to respond in a timely manner according to the needs. However, sports only as a sports, unique and cannot get a long-term rapid development. "Smart" sports can easily find venues for people, monitor people's sports behavior, and formulate matching exercise prescriptions for them. Moreover, it can better combine sports with health, culture, tourism, etc., so as to better integrate life services, urbanization process, etc., and make sports in line with the times. In this paper, the artificial intelligence-assisted agile Internet of Things is used to study the sports simulation scheme, and an intelligent sports simulation system is constructed. The experimental research results show that the sports simulation system based on artificial intelligence-assisted agile Internet of Things proposed in this paper has a good performance in sports simulation.

Shuping Xu, <https://orcid.org/0009-0000-0252-5204>

Long Wang, <https://orcid.org/0009-0003-8951-1842>

REFERENCES

- [1] Aso, K.; Hwang, D. H.; Koike, H.: Portable 3D Human Pose Estimation for Human-Human Interaction using a Chest-Mounted Fisheye Camera, In Augmented Humans Conference 2021, 2021, (pp. 116-120). <https://doi.org/10.1145/3458709.3458986>
- [2] Díaz, R. G.; Laamarti, F.; El Saddik, A.: DTCoach: Your Digital Twin Coach on the Edge During COVID-19 and Beyond, IEEE Instrumentation & Measurement Magazine, 24(6), 2021, 22-28. <https://doi.org/10.1109/MIM.2021.9513635>
- [3] Ershadi-Nasab, S.; Noury, E.; Kasaei, S.; Sanaei, E.: Multiple human 3d pose estimation from multiview images, Multimedia Tools and Applications, 77(12), 2018 , 15573-15601. <https://doi.org/10.1007/s11042-017-5133-8>
- [4] Gu, R.; Wang, G.; Jiang, Z.; Hwang, J. N.: Multi-person hierarchical 3d pose estimation in natural videos, IEEE Transactions on Circuits and Systems for Video Technology, 30(11), 2019, 4245-4257. <https://doi.org/10.1109/TCSVT.2019.2953678>
- [5] Hua, G.; Li, L.; Liu, S.: Multipath affinity stacked—hourglass networks for human pose estimation, Frontiers of Computer Science, 14(4), 2020, 1-12. <https://doi.org/10.1007/s11704-019-8266-2>
- [6] Li, M.; Zhou, Z.; Liu, X.: Multi-person pose estimation using bounding box constraint and LSTM. IEEE Transactions on Multimedia, 21(10), 2019, 2653-2663. <https://doi.org/10.1109/TMM.2019.2903455>
- [7] Liu, S.; Li, Y.; Hua, G.: Human pose estimation in video via structured space learning and halfway temporal evaluation, IEEE Transactions on Circuits and Systems for Video Technology, 29(7), 2018, 2029-2038. <https://doi.org/10.1109/TCSVT.2018.2858828>
- [8] Martínez-González, A.; Villamizar, M.; Canévet, O.; Odobez, J. M.: Efficient convolutional neural networks for depth-based multi-person pose estimation, IEEE Transactions on Circuits and Systems for Video Technology, 30(11), 2019, 4207-4221. <https://doi.org/10.1109/TCSVT.2019.2952779>
- [9] McNally, W.; Wong, A.; McPhee, J.: Action recognition using deep convolutional neural networks and compressed spatio-temporal pose encodings, Journal of Computational Vision and Imaging Systems, 4(1), 2018, 3-3.
- [10] Mehta, D.; Sridhar, S.; Sotnychenko, O.; Rhodin, H.; Shafiei, M.; Seidel, H. P.; Theobalt, C.: Vnect: Real-time 3d human pose estimation with a single rgb camera, ACM Transactions on Graphics (TOG), 36(4), 2017 , 1-14. <https://doi.org/10.1145/3072959.3073596>

- [11] Nasr, M.; Ayman, H.; Ebrahim, N.; Osama, R.; Mosaad, N.; Mounir, A.: Realtime Multi-Person 2D Pose Estimation, *International Journal of Advanced Networking and Applications*, 11(6), 2020 , 4501-4508. <https://doi.org/10.35444/IJANA.2020.11069>
- [12] Nie, X.; Feng, J.; Xing, J.; Xiao, S.; Yan, S.: Hierarchical contextual refinement networks for human pose estimation, *IEEE Transactions on Image Processing*, 28(2), 2018, 924-936. <https://doi.org/10.1109/TIP.2018.2872628>
- [13] Nie, Y.; Lee, J.; Yoon, S.; Park, D. S.: A Multi-Stage Convolution Machine with Scaling and Dilation for Human Pose Estimation, *KSII Transactions on Internet and Information Systems (TIIS)*, 13(6), 2019, 3182-3198. <https://doi.org/10.3837/tiis.2019.06.023>
- [14] Petrov, I.; Shakhuro, V.; Konushin, A.: Deep probabilistic human pose estimation, *IET Computer Vision*, 12(5), 2018, 578-585. <https://doi.org/10.1049/iet-cvi.2017.0382>
- [15] Szűcs, G.; Tamás, B: Body part extraction and pose estimation method in rowing videos, *Journal of computing and information technology*, 26(1), 2018, 29-43. <https://doi.org/10.20532/cit.2018.1003802>
- [16] Thành, N. T.; Công, P. T.: An Evaluation of Pose Estimation in Video of Traditional Martial Arts Presentation, *Journal of Research and Development on Information and Communication Technology*, 2019(2), 2019, 114-126. <https://doi.org/10.32913/mic-ict-research.v2019.n2.864>
- [17] Xu, J.; Tasaka, K.; Yamaguchi, M.: Fast and Accurate Whole-Body Pose Estimation in the Wild and Its Applications, *ITE Transactions on Media Technology and Applications*, 9(1), 2021, 63-70. <https://doi.org/10.3169/mta.9.63>
- [18] Zarkeshev, A.; Csiszár, C.: Rescue Method Based on V2X Communication and Human Pose Estimation, *Periodica Polytechnica Civil Engineering*, 63(4), 2019, 1139-1146. <https://doi.org/10.3311/PPci.13861>